

Specific aromatic foldamers potently inhibit spontaneous and seeded A β 42 and A β 43 fibril assembly

Katelyn M. Seither*, Heather A. McMahon*, Nikita Singh*, Hejia Wang*, Mimi Cushman-Nick*^{†‡}, Geronda L. Montalvo*[§], William F. DeGrado[‡] and James Shorter*^{†§1}

*Department of Biochemistry and Biophysics, Perelman School of Medicine at the University of Pennsylvania, 805b Stellar-Chance Laboratories, 422 Curie Boulevard, Philadelphia, PA 19104, U.S.A.

[†]Neuroscience Graduate Group, Perelman School of Medicine at the University of Pennsylvania, 805b Stellar-Chance Laboratories, 422 Curie Boulevard, Philadelphia, PA 19104, U.S.A.

[‡]Department of Pharmaceutical Chemistry, University of California, San Francisco, CVRI-MC Box 3122, San Francisco, CA 94158-9001 U.S.A.

[§]Biochemistry and Molecular Biophysics Graduate Group, Perelman School of Medicine at the University of Pennsylvania, 805b Stellar-Chance Laboratories, 422 Curie Boulevard, Philadelphia, PA 19104, U.S.A.

Amyloid fibrils are self-propagating entities that spread pathology in several devastating disorders including Alzheimer's disease (AD). In AD, amyloid- β (A β) peptides form extracellular plaques that contribute to cognitive decline. One potential therapeutic strategy is to develop inhibitors that prevent A β misfolding into proteotoxic conformers. Here, we design specific aromatic foldamers, synthetic polymers with an aromatic salicylamide (Sal) or 3-amino benzoic acid (Benz) backbone, short length (four repetitive units), basic arginine (Arg), lysine (Lys) or citrulline (Cit) side chains, and various N- and C-terminal groups that prevent spontaneous and seeded A β fibrillization. Ac-Sal-(Lys-Sal)₃-CONH₂ and Sal-(Lys-Sal)₃-CONH₂ selectively inhibited A β 42 fibrillization, but were ineffective against A β 43, an overlooked species that is highly neurotoxic and frequently deposited in AD brains. By contrast, (Arg-Benz)₄-CONH₂ and

(Arg-Sal)₃-(Cit-Sal)-CONH₂ prevented spontaneous and seeded A β 42 and A β 43 fibrillization. Importantly, (Arg-Sal)₃-(Cit-Sal)-CONH₂ inhibited formation of toxic A β 42 and A β 43 oligomers and proteotoxicity. None of these foldamers inhibited Sup35 prionogenesis, but Sal-(Lys-Sal)₃-CONH₂ delayed aggregation of fused in sarcoma (FUS), an RNA-binding protein with a prion-like domain connected with amyotrophic lateral sclerosis and frontotemporal dementia. We establish that inhibitors of A β 42 fibrillization do not necessarily inhibit A β 43 fibrillization. Moreover, (Arg-Sal)₃-(Cit-Sal)-CONH₂ inhibits formation of toxic A β conformers and seeding activity, properties that could have therapeutic utility.

Key words: Alzheimer's disease, amyloid, A β 42 (amyloid- β 42), A β 43 (amyloid- β 43), foldamer, protein misfolding.

INTRODUCTION

Protein misfolding can be fatal [1,2]. Proteins misfold from soluble species into highly stable, cross- β amyloid fibrils in Alzheimer's disease (AD) and several other neurodegenerative diseases [1,2]. One strategy to combat these disorders is to develop small molecules that inhibit amyloidogenesis and prevent toxic protein misfolding [3–6]. Although daunting challenges face potential small molecule inhibitors of amyloidogenesis [7], they are beginning to reach the clinic. Indeed, tafamidis, a small molecule inhibitor of transthyretin amyloidogenesis treats familial amyloid polyneuropathy, a rare but deadly disease [8,9].

Here, we focus on amyloid- β (A β) peptides, A β 42 and A β 43, which form amyloid fibrils and accumulate in extracellular plaques that are a hallmark of AD [10–16]. AD is a progressive neurodegenerative disease and the most common cause of dementia worldwide [12]. Aging is a significant risk factor for AD and there are no effective therapies [11]. In A β biogenesis, the full-length transmembrane amyloid precursor protein (APP) undergoes sequential cleavage by β - and γ -secretase, resulting in peptides that are 38–43 amino acids in length [10,12]. A β 42 and A β 40 are most commonly associated with AD pathology

[10–12]. A β 40 is a more benign, perhaps even neuroprotective species [17,18], which slowly assembles into amyloid fibrils. By contrast, A β 42 oligomerizes and fibrillizes more rapidly due to two additional C-terminal residues that introduce additional steric zipper hexapeptides that drive assembly [19–21].

Although A β peptides longer than A β 42 are found in AD, they are not a major species and their pathogenic role has been ignored. Recently, this view has changed. A β 43 is a potent contributor to neurotoxicity in AD [13–15]. A β 43 contains an additional threonine residue at the C-terminal end and fibrillizes more rapidly than A β 42 [13]. A β 43 is more abundant in insoluble fractions than A β 40 in AD and its presence in senile plaques is directly correlated with cognitive decline [13–16]. Specific inhibitors of A β 43 misfolding have not been identified and it is unclear whether inhibitors of A β 42 misfolding will also inhibit A β 43 misfolding.

A β monomers form amyloid via nucleated conformational conversion [22]. First, a subpopulation of A β monomers forms molten oligomers, which gradually rearrange into amyloidogenic oligomers that nucleate cross- β fibrils [22,23]. Rearrangement is rate limiting and causes the lag phase of spontaneous fibrillization [22]. During lag phase, A β forms diverse oligomeric species, which can be highly toxic [21,24–27]. Upon nucleation, fibrils

Abbreviations: AD, Alzheimer's disease; A β , amyloid- β ; Benz, 3-amino benzoic acid; DCM, dichloromethane; DIEA, di-isopropylethylamine; DMEM, Dulbecco's modified Eagle's medium; DMF, dimethylformamide; EGCG, (–)-epigallocatechin-3-gallate; HFIP, 1,1,1,3,3,3-hexafluoro-2-propanol; LDH, lactate dehydrogenase; MeOH, methanol; NM, N-terminal and middle domains of Sup35; Sal, salicylamide; TEV, tobacco etch virus; ThT, thioflavin-T.

¹ To whom correspondence should be addressed (email jshorter@mail.med.upenn.edu).

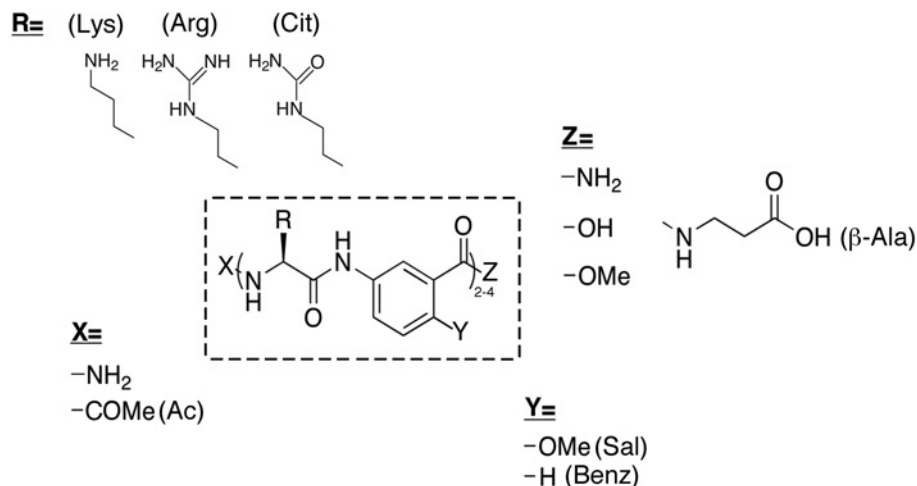


Figure 1 Overview of aromatic foldamer structure

The core foldamer structure is shown in the dashed box, which can be decorated with different moieties at X-, R-, Y- and Z-positions indicated on the periphery. Foldamers possess an aromatic Sal or Benz backbone (Y = OMe or H), Arg, Lys or Cit side chains (R = Arg, Lys or Cit), short length (two to four repetitive units) and various N- (X = NH₂ or Ac) and C- (Z = NH₂, OH, OMe or β-Ala) terminal groups.

rapidly grow via their self-templating ends, which convert Aβ conformers into the cross-β conformation [20,28]. When coupled to fibril fragmentation, this ‘seeding’ activity enables Aβ fibrils to become self-propagating agents that transmit pathology and disease [1,29–31]. Aβ fibrils also provide catalytic surfaces for ‘secondary’ nucleation events distinct from fibril elongation [32–34]. Here, lateral Aβ fibril surfaces convert Aβ monomers into toxic oligomers [32–34]. Thus, formation of toxic oligomers and fibrils is intimately linked [32–34]. These secondary nucleation events also help explain Aβ assembly kinetics [32–34]. Aβ forms different cross-β fibril structures termed ‘strains’, which can differ in toxicity and cause distinct brain pathology [35–38]. Aβ fibrils are usually less toxic than pre-amyloid oligomers [21,39]. However, Aβ fibrils also display toxicity [6,35,36,39]. A key challenge is to manipulate Aβ assembly in a manner that depopulates toxic conformers [7]. Agents that inhibit seeded assembly hold promise for preventing the spread of Aβ pathology in AD.

Numerous potential inhibitors of Aβ misfolding have been explored, including small molecules, peptides, molecular chaperones, protein disaggregases and antibodies [3,6,39–45]. In the present study, we explore a different strategy by pursuing foldamers; non-biological discrete chain molecules that lack a canonical peptide backbone but can fold into specific structures [46]. Foldamers have been utilized as antimicrobial agents and molecular scaffolds [47–50]. Peptides containing non-natural amino acids, similar to foldamers, have been useful for understanding the misfolding of various amyloidogenic peptides [42,51–53]. Foldamers have several advantageous properties that could make them a valuable class of amyloid inhibitors. Due to their semi-rigid backbone, foldamers can assume an organized conformation at low entropic cost with relatively few monomeric units [50,54]. Compared with α peptides, foldamers have greater thermodynamic stability and resist proteases. Furthermore, foldamers of varying lengths with diverse side chains and 3D shapes can be synthesized. These features enable foldamer design for interaction with diverse biological targets [47–50,55]. In the present study, we explore aromatic foldamers as antagonists of Aβ₄₂ and Aβ₄₃ amyloidogenesis.

MATERIALS AND METHODS

Generation of soluble and fibrillar Aβ₄₂ and Aβ₄₃

To produce monomeric Aβ, synthetic lyophilized Aβ₄₂ or Aβ₄₃ (W.M. Keck Facility, Yale University) was dissolved in 1,1,1,3,3,3-hexafluoro-2-propanol (HFIP, Sigma) at 2 mg/ml. HFIP was removed by drying in a speed vacuum for 30 min. The resulting peptide film was dissolved in DMSO to 1 mM. Aβ₄₂ or Aβ₄₃ fibrils for seeding experiments were prepared by diluting monomeric Aβ₄₂ or Aβ₄₃ in KHMD (150 mM KCl, 40 mM HEPES-KOH pH 7.4, 20 mM MgCl₂ and 1 mM DTT) to 10 μM. This solution was incubated at 37°C for 3–5 days with agitation (700 r.p.m.) in an Eppendorf Thermomixer. For seeding experiments, preformed fibrils were briefly sonicated or vortex-mixed prior to use. We also prepared Aβ₄₂ or Aβ₄₃ using a protocol that avoids DMSO. Thus, Aβ₄₂ or Aβ₄₃ was dissolved in HFIP followed by evaporation of the solvent to dryness [56]. Dry peptide films were dissolved in a minimal volume of 60 mM NaOH followed by dilution with deionized water and sonication for 1 min using a bath sonicator. Peptides were diluted to 0.2 mM by adding an equal volume of 20 mM sodium phosphate buffer (PB, Sigma), pH 8 plus 0.2 mM EDTA (PBE). Samples were centrifuged at 16000 g for 3 min and subjected to Superdex 75 gel filtration in PBE to remove residual solvent.

Foldamers

Foldamers (Lys-Sal)₄-CONH₂, (Arg-Benz)₄-CONH₂, (Lys-Sal)₄-COMe, (Lys-Sal)₄-COOH, (Lys-Sal)₄-COβAla, Ac-(Lys-Sal)₃-CONH₂, Sal-(Lys-Sal)₃-CONH₂ and Ac-Sal-(Lys-Sal)₃-CONH₂ (where Sal is salicylamide and Benz is 3-amino benzoic acid) were from PolyMedix and were dissolved in TBS (50 mM Tris/HCl pH 7.4, 150 mM NaCl) to obtain concentrated stock solutions. Foldamers (Cit-Sal)₄-CONH₂, (Arg-Sal)₂-(Cit-Sal)-(Arg-Sal)-CONH₂, (Arg-Sal)₃-(Cit-Sal)-CONH₂, (Cit-Sal)₂-(Arg-Sal)-(Cit-Sal)-CONH₂, (Cit-Sal)-(Arg-Sal)-(Cit-Sal)₂-CONH₂ and (Arg-Sal-Cit-Sal)₂-CONH₂ were also from PolyMedix. These foldamers were dissolved in 1:1 TBS/DMSO to obtain

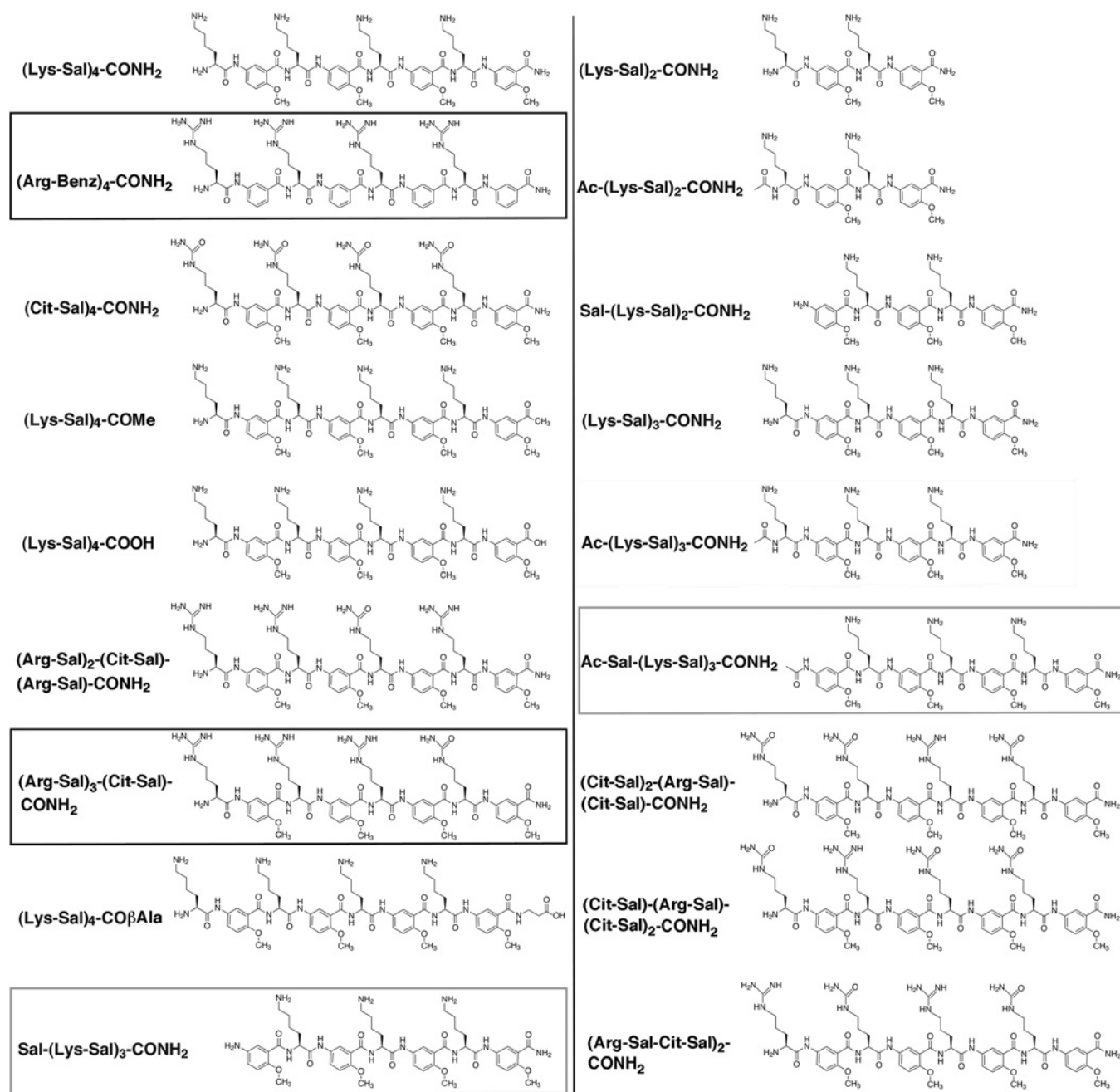


Figure 2 Nomenclature and structure of aromatic foldamers

Three-letter amino acid nomenclature is used to indicate the side chain (Lys, Arg or Cit) and the Sal or Benz backbone is indicated. N- (Ac) and C- (NH₂, OH, OMe or β-Ala) terminal groups are also indicated. Foldamers that inhibit spontaneous Aβ₄₂ and Aβ₄₃ fibrillization, (Arg-Benz)₄-CONH₂ and (Arg-Sal)₃-(Cit-Sal)-CONH₂, are boxed in black. Foldamers that inhibit spontaneous Aβ₄₂ fibrillization but not spontaneous Aβ₄₃ fibrillization, Sal-(Lys-Sal)₃-CONH₂ and Ac-Sal-(Lys-Sal)₃-CONH₂, are boxed in grey.

concentrated stocks. Subsequent dilutions were made from these stocks to appropriate concentrations in KHMD or PBE.

Foldamers (Lys-Sal)₂-CONH₂, Ac-(Lys-Sal)₂-CONH₂, Sal-(Lys-Sal)₂-CONH₂, (Lys-Sal)₃-CONH₂ and Ac-(Lys-Sal)₃-CONH₂ were synthesized at room temperature on a 100 μmol scale using rink amide resin (GemScript Corporation, 0.6 mmol/g substitution) for support of alternating α- (Bachem) and aromatic amino acids. Resin was swelled in 100% dimethylformamide (DMF, Fisher Scientific) for 1 h, followed by a 30 min deprotection using 5% piperazine (Sigma-Aldrich) in DMF.

The first residue was coupled to the resin using 3 equiv. of amino acid, 2.8 equiv. of 2-(6-chloro-1H-benzotriazole-1-yl)-1,1,3,3-tetramethylammonium hexafluorophosphate (HCTU, GL Biosciences) activator and 7.5 equiv. of di-isopropylethylamine (DIEA, CHEM-IMPEX International), shaking for 1 h at room temperature. The resin was washed three times each with DMF, dichloromethane (DCM, Fisher Scientific) and DMF. This step was followed by deprotection (as above). Coupling and deprotection steps were cycled for the remaining residues in each respective peptide sequence. After deprotection of the

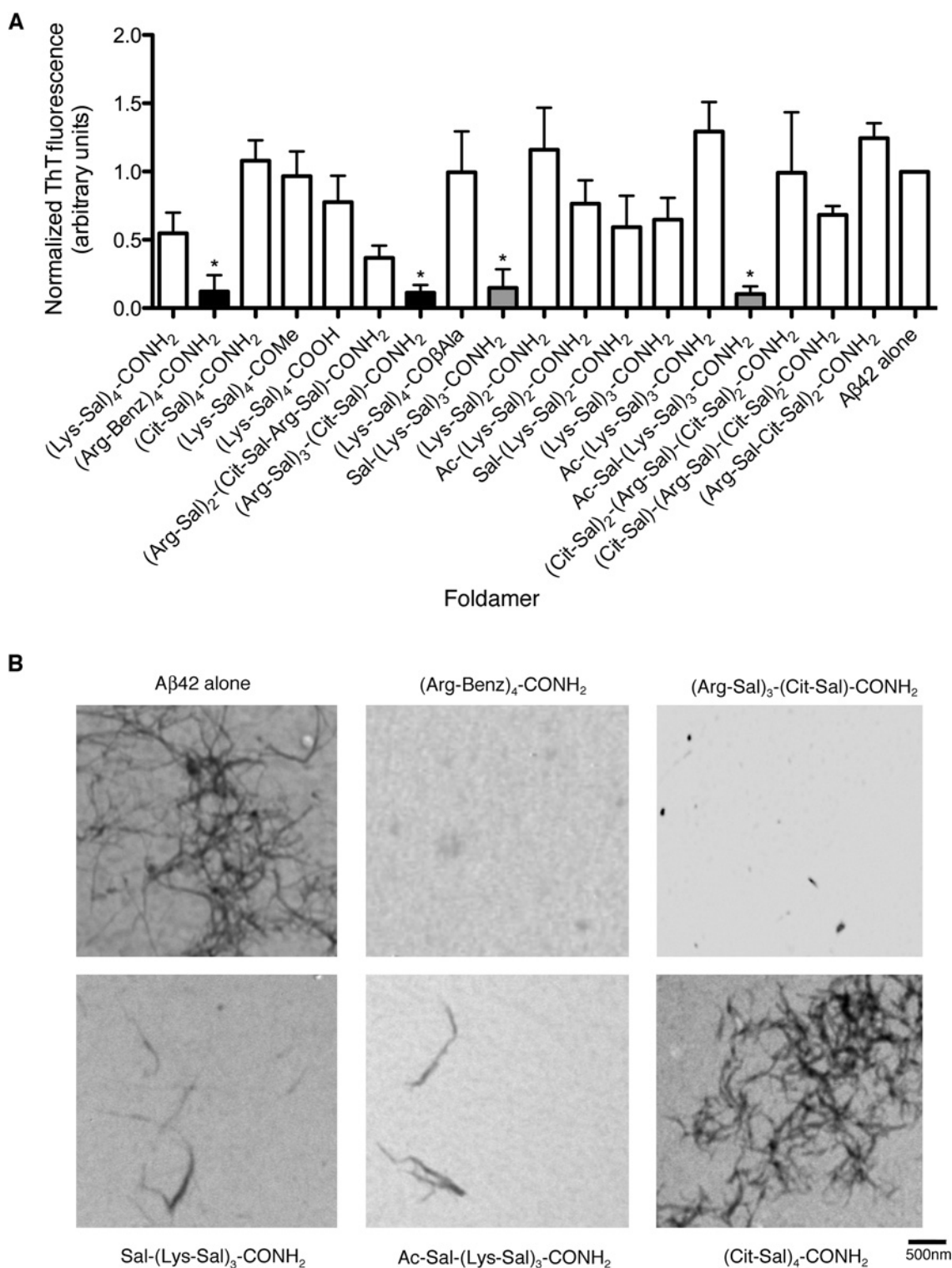


Figure 3 (Arg-Benz)₄-CONH₂, (Arg-Sal)₃-(Cit-Sal)-CONH₂, Sal-(Lys-Sal)₃-CONH₂ and Ac-Sal-(Lys-Sal)₃-CONH₂ inhibit spontaneous Aβ42 fibrillization

(A) Aβ42 (5 μM) was incubated with agitation for 8 h at 25°C plus or minus the indicated foldamer (10 μM). Aβ42 fibrillization was assessed by ThT fluorescence. Values represent means ± S.E.M. ($n = 3-6$). A one-way ANOVA with the post-hoc Dunnett's multiple comparisons test was used to compare Aβ42 alone to each Aβ42 plus foldamer condition (* denotes $P < 0.05$). Foldamers that selectively inhibit Aβ42 fibrillization are indicated by grey bars and foldamers that inhibit Aβ42 and Aβ43 fibrillization are indicated by black bars. (B) Aβ42 (5 μM) was incubated with agitation for 4 h at 25°C in the absence or presence of the indicated foldamer (10 μM). Aβ42 fibrillization was assessed by EM. Scale bar, 500 nm.

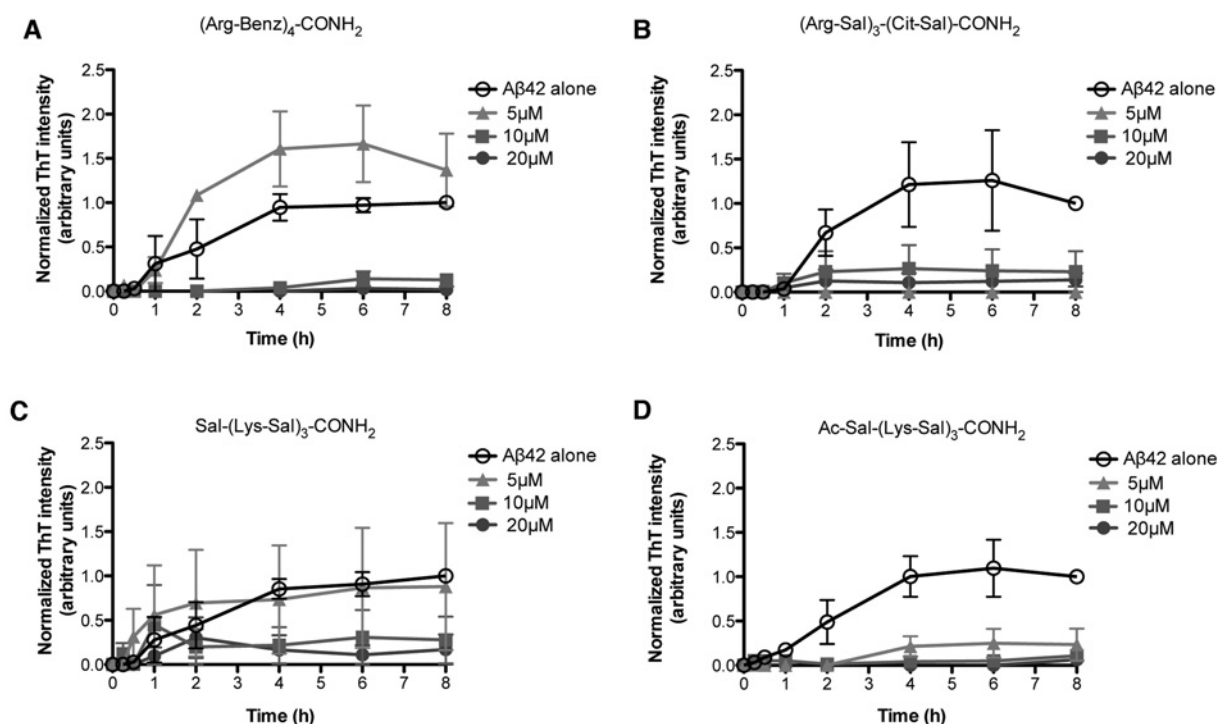


Figure 4 Effect of inhibitory foldamers on spontaneous A β 42 fibrillization kinetics

(A–D) A β 42 (5 μ M) was incubated with agitation for 0–8 h at 25 $^{\circ}$ C in the absence (open circles) or presence of 5 μ M (filled triangles), 10 μ M (filled squares) or 20 μ M (filled circles) (Arg-Benz) $_4$ -CONH $_2$ (A), (Arg-Sal) $_3$ -(Cit-Sal)-CONH $_2$ (B), Sal-(Lys-Sal) $_3$ -CONH $_2$ (C) or Ac-Sal-(Lys-Sal) $_3$ -CONH $_2$ (D). A β 42 fibrillization was assessed by ThT fluorescence. Values represent means \pm S.E.M. ($n = 3$).

final residue the product was rinsed [three times with DMF, three times with DCM, three times with DMF and three times with methanol (MeOH)] and dried with MeOH. This product was split in half. The first half was re-swelled in DMF and acetylated by incubating the resin in 5% acetic anhydride in 2.5% DIEA and 92.5% DMF for 10 min. This acetylated portion was rinsed and dried (as above). Next, both halves (one with a N-terminal acetyl and a second with a N-terminal free amide) were cleaved from the resin using a cocktail of 2:2:2:94 H $_2$ O/TIS (tri-isopropyl silane)/anisole/TFA (trifluoroacetic acid; Sigma-Aldrich) for 2 h at room temperature. The peptide solution was filtered from the resin and precipitated using 1:1 cold ethyl ether:hexane. The precipitate was dried by lyophilization. The mass and purity of each product was verified by MALDI-TOF MS (Bruker microflex LRF) and analytical HPLC (C18 column). Dried crude foldamer was purified by preparative reverse-phase HPLC, dried by lyophilization and mass and purity was verified as above. All samples were prepared by directly dissolving lyophilized foldamer into TBS buffer to 2 mM.

Spontaneous and seeded A β 42, A β 43 and N-terminal and middle domain of Sup35 (NM) fibrillization

For spontaneous fibrillization, soluble A β 42 or A β 43 (1 mM) in DMSO was diluted to 5 μ M in KHMD containing 25 μ M thioflavin-T (ThT) plus or minus foldamer (0–20 μ M). For seeded fibrillization, preformed A β 42 or A β 43 fibrils (10 μ M monomer) were added at a final concentration of 0.1 μ M (monomer). Alternatively, A β 42 or A β 43 were prepared using just HFIP and were assembled at 5 μ M in PBE containing 25 μ M ThT plus or minus foldamer (20 μ M). NM was purified as described [57]. NM (5 μ M) was assembled in KHMD containing

25 μ M ThT plus or minus foldamer (20 μ M). For seeded fibrillization, preformed NM fibrils (5 μ M monomer) were added at a final concentration of 0.1 μ M (monomer). Reactions were conducted in 96-well plates and incubated at 25 $^{\circ}$ C in a TECAN Safire II plate reader (Tecan USA) for up to 8 h with agitation. ThT fluorescence was measured at the indicated times. The excitation wavelength was 450 nm (5 nm bandwidth) and the emission wavelength was 482 nm (10 nm bandwidth). ThT fluorescence values reported are arbitrary and are normalized to the final assembly time point of the A β alone condition.

FUS aggregation

GST-TEV-FUS was purified as described [58]. Aggregation was initiated by addition of tobacco etch virus (TEV) protease to GST-TEV-FUS (5 μ M) plus or minus foldamer (20 μ M) in assembly buffer (50 mM Tris/HCl pH 8, 0.2 M trehalose and 20 mM glutathione). Aggregation was for 0–90 min at 25 $^{\circ}$ C without agitation in a 96-well plate and was assessed by turbidity (absorbance at 395 nm) using a Tecan Infinite M1000 plate reader [58]. No aggregation occurred unless TEV protease was added to separate GST from FUS [58]. SDS/PAGE and Coomassie staining revealed that foldamers did not inhibit cleavage of GST-TEV-FUS by TEV.

Electron microscopy

Reactions were adhered on to 300-mesh-formvar carbon-coated EM grids overnight before being negatively stained with 2% uranyl acetate for 2 min and rinsed with milli-Q distilled water. Micrographs were acquired using a JEOL 1010 TEM (Jeol USA).

Tracking A11-reactive A β 42 or A β 43 conformers

The oligomer-specific A11 antibody was used to detect toxic A β 42 or A β 43 oligomers by ELISA as described [21]. Foldamers did not cross-react with A11.

Toxicity assays

SH-SY5Y human neuroblastoma cells were maintained in Dulbecco's modified Eagle's medium (DMEM) plus 10 mM Hepes, 10% FBS, 4 mM glutamine, penicillin (200 units/ml) and streptomycin (200 μ g/ml) in 5% CO₂ at 37°C. Cells were differentiated in serum-free DMEM with N2 supplement and 10 μ M all-*trans*-retinoic acid before use. Cells were plated at (10000 cells/well) in 96-well plates and grown overnight. Medium was removed and A β conformers or controls were added and cells were incubated for 24 h at 37°C. Toxicity was assessed using an MTT kit (Tox-1; Sigma) or via lactate dehydrogenase (LDH) release using the CytoTox-ONE™ kit (Promega). Toxicity values were normalized to the buffer control without A β .

RESULTS AND DISCUSSION

Rationale and foldamer design

As potential inhibitors of A β 42 and A β 43 amyloidogenesis, we explored aromatic foldamers (Figures 1 and 2). Some of these foldamers were originally synthesized as inhibitors of heparin and are rich in aromatic and positively charged groups [55]. They possess an aromatic salicylamide (Sal) or 3-amino benzoic acid (Benz) backbone (Figure 1; Y = OMe or H), lysine (Lys), arginine (Arg) or citrulline (Cit) side chains (Figure 1; R = Lys, Arg or Cit), short length (two to four repetitive units) (Figure 1) and various N- (Figure 1; X = NH₂ or COMe [Ac]) and C- (Figure 1; Z = NH₂, OH, OMe or β -Ala) terminal groups. We selected this design for four reasons. First, the aromatic backbone is similar to ones employed by Nowick et al. [42,51–53] in protein aggregation inhibitors. Secondly, interactions between aromatic residues within short amyloidogenic peptides mediate molecular recognition during fibrillization [59]. Moreover, polyphenols such as (–)-epigallocatechin-3-gallate (EGCG) inhibit amyloidogenesis and prevent cytotoxicity [57,59–61]. Thus, the aromatic foldamer spine might antagonize aromatic interactions critical for fibrillization. Thirdly, the aromatic foldamers investigated are approximately the same length (two to four repetitive units) as steric zipper hexapeptides that form amyloid [19]. Finally, basic side chains, particularly arginine exert hydrotropic effects and prevent protein aggregation [62].

Foldamer inhibition screen

We tested 18 aromatic foldamers (Figure 2) for inhibition of spontaneous (i.e. in the absence of preformed fibrils) A β 42 fibrillization. The majority of foldamers did not significantly inhibit A β 42 fibrillization (Figure 3A). However, (Arg-Benz)₄-CONH₂, (Arg-Sal)₃-(Cit-Sal)-CONH₂, Sal-(Lys-Sal)₃-CONH₂ and Ac-Sal-(Lys-Sal)₃-CONH₂ were strong inhibitors (Figure 2 boxed in black or grey; Figures 3A and 3B; Figures 4A–4D). (Arg-Sal)₃-(Cit-Sal)-CONH₂ was the most potent with an IC₅₀ of ~1.6 μ M.

Several important foldamer properties emerge for inhibition of A β 42 fibrillization. First, a foldamer must have a backbone with at least four aromatic units to antagonize A β 42 fibrillization. Thus, (Lys-Sal)₂-CONH₂, Ac-(Lys-Sal)₂-CONH₂, Sal-(Lys-Sal)₂-CONH₂, (Lys-Sal)₃-CONH₂ and Ac-(Lys-Sal)₃-

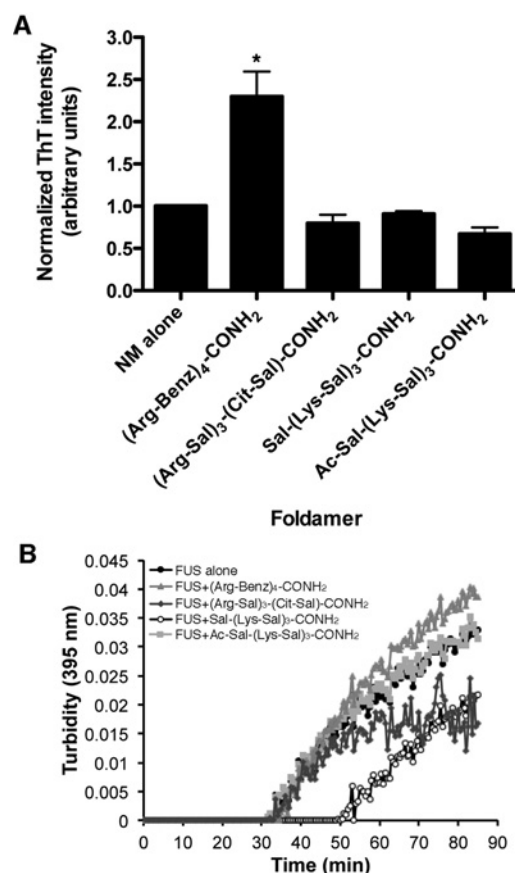


Figure 5 Sal-(Lys-Sal)₃-CONH₂ has no effect on NM fibrillization but delays FUS aggregation

(A) NM (5 μ M) was incubated with agitation for 4 h at 25°C plus or minus the indicated foldamer (20 μ M). NM fibrillization was assessed by ThT fluorescence. Values represent means \pm S.E.M. ($n = 3$). A one-way ANOVA with the *post-hoc* Dunnett's multiple comparisons test was used to compare NM alone to each NM plus foldamer condition (* denotes $P < 0.05$). (B) GST-FUS (5 μ M) was incubated in the presence of the indicated foldamer (20 μ M) plus TEV protease at 25°C for 0–90 min. Turbidity measurements (absorbance at 395 nm) were taken every minute to assess aggregation. A representative dataset is shown.

CONH₂ failed to inhibit assembly (Figures 2 and 3A). Secondly, foldamers with more than three lysine or citrulline side chains were ineffective, encompassing: (Lys-Sal)₄-CONH₂, (Cit-Sal)₄-CONH₂, (Lys-Sal)₄-COMe, (Lys-Sal)₄-COOH and (Lys-Sal)₄-CO β Ala (Figures 2 and 3A). By contrast, Sal-(Lys-Sal)₃-CONH₂ and Ac-Sal-(Lys-Sal)₃-CONH₂, which possess three lysine side chains and four aromatic backbone units, were potent inhibitors (Figures 2 and 3A). Thirdly, foldamers with three or more consecutive Arg side chains were effective inhibitors. Thus, (Arg-Benz)₄-CONH₂ and (Arg-Sal)₃-(Cit-Sal)-CONH₂ were potent inhibitors, whereas (Arg-Sal)₂-(Cit-Sal)-(Arg-Sal)-CONH₂, (Cit-Sal)₂-(Arg-Sal)-(Cit-Sal)-CONH₂, (Cit-Sal)-(Arg-Sal)-(Cit-Sal)₂-CONH₂ and (Arg-Sal-Cit-Sal)₂-CONH₂ were ineffective (Figures 2 and 3A).

Select small molecules that inhibit A β 42 fibrillization also disassemble A β 42 fibrils [4,57,60]. However, even when present in 4-fold molar excess, (Arg-Benz)₄-CONH₂, (Arg-Sal)₃-(Cit-Sal)-CONH₂, Sal-(Lys-Sal)₃-CONH₂ and Ac-Sal-(Lys-Sal)₃-CONH₂ did not disassemble A β 42 fibrils after 24 h (results not shown). Thus, these foldamers do not reverse A β 42 fibrillization.

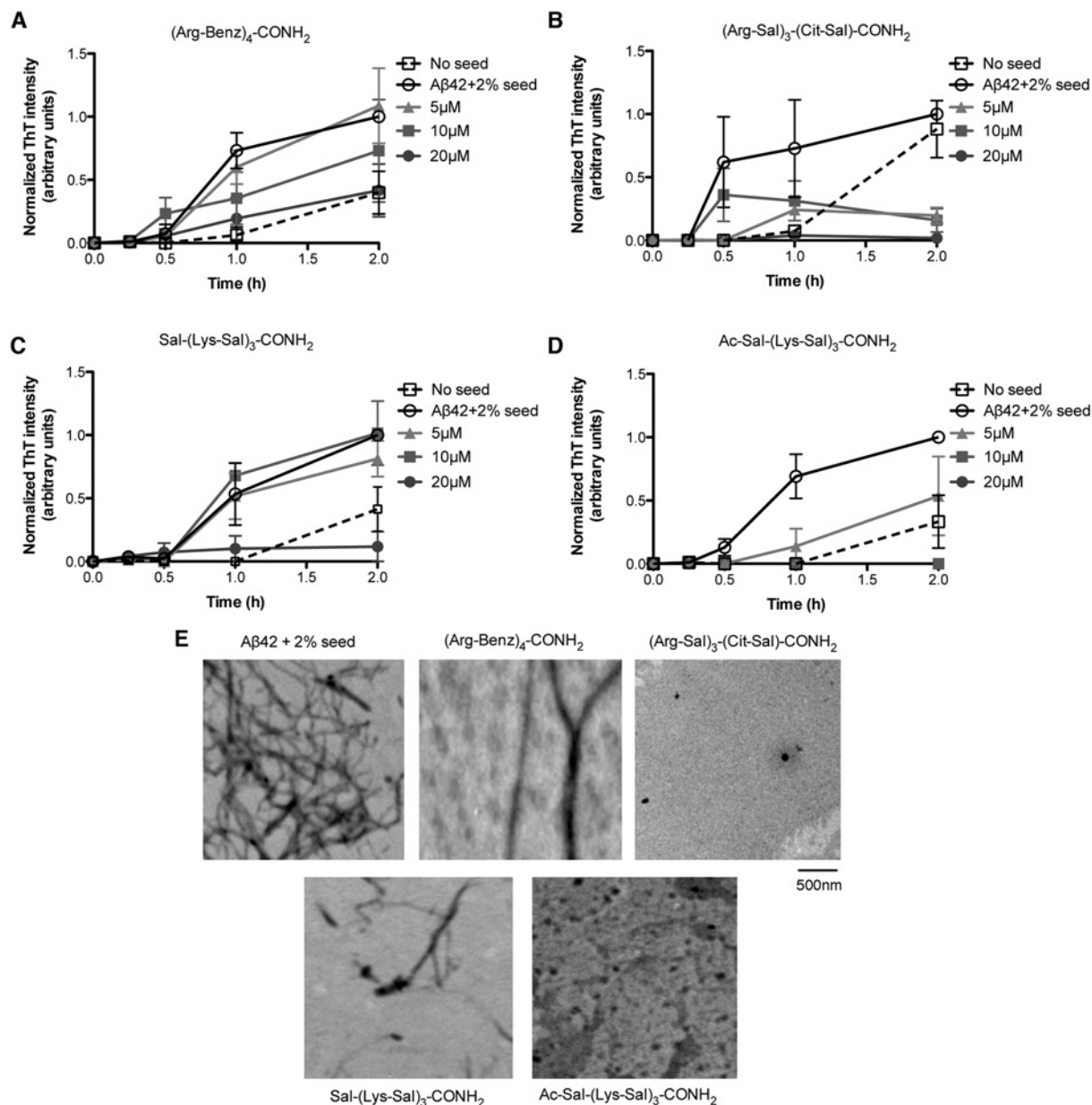


Figure 6 (Arg-Sal)₃-(Cit-Sal)-CONH₂ and Ac-Sal-(Lys-Sal)₃-CONH₂ inhibit seeded A β 42 fibrillization

(A–D) A β 42 (5 μ M) was incubated with agitation for 0–2 h at 25 °C without (open squares) or with A β 42 fibril seed (0.1 μ M monomer) in the absence (open circles) or presence of 5 μ M (filled triangles), 10 μ M (filled squares) or 20 μ M (filled circles) (Arg-Benz)₄-CONH₂ (A), (Arg-Sal)₃-(Cit-Sal)-CONH₂ (B), Sal-(Lys-Sal)₃-CONH₂ (C) or Ac-Sal-(Lys-Sal)₃-CONH₂ (D). A β 42 fibrillization was assessed by ThT fluorescence. Values represent means \pm S.E.M. ($n = 3$). (E) A β 42 (5 μ M) plus A β 42 fibril seed (0.1 μ M monomer) was incubated with agitation for 4 h at 25 °C plus or minus the indicated foldamer (10 μ M). A β 42 fibrillization was assessed by EM. Scale bar, 500 nm.

Foldamers that inhibit A β 42 fibrillization do not inhibit NM fibrillization

Next, we assessed foldamer specificity by testing whether they inhibited amyloidogenesis of the prion domain, NM, of yeast Sup35 [63]. (Arg-Benz)₄-CONH₂, (Arg-Sal)₃-(Cit-Sal)-CONH₂, Sal-(Lys-Sal)₃-CONH₂ and Ac-Sal-(Lys-Sal)₃-CONH₂ did not inhibit NM fibrillization (Figure 5A). In the presence of (Arg-Benz)₄-CONH₂, NM formed fibrils that exhibited greater ThT fluorescence (Figure 5A). EM revealed that purely NM fibrils formed in the presence or absence of (Arg-Benz)₄-CONH₂ and sedimentation analysis revealed that equal quantities of NM formed fibrils (results not shown). Thus, (Arg-Benz)₄-CONH₂ does not

stimulate NM fibrillization. Rather, we suggest that NM accesses a different prion strain in the presence of (Arg-Benz)₄-CONH₂. NM accesses different prion strains in the presence of certain small molecules, such as EGCG [57,63]. None of these foldamers inhibited seeded NM fibrillization (results not shown). Thus, these foldamers are not generic inhibitors of amyloidogenesis.

Sal-(Lys-Sal)₃-CONH₂ delays FUS aggregation

To further test specificity, we assessed inhibition of aggregation of FUS, an RNA-binding protein with a prion-like domain, which is connected with amyotrophic lateral sclerosis and frontotemporal dementia [1,58,64].

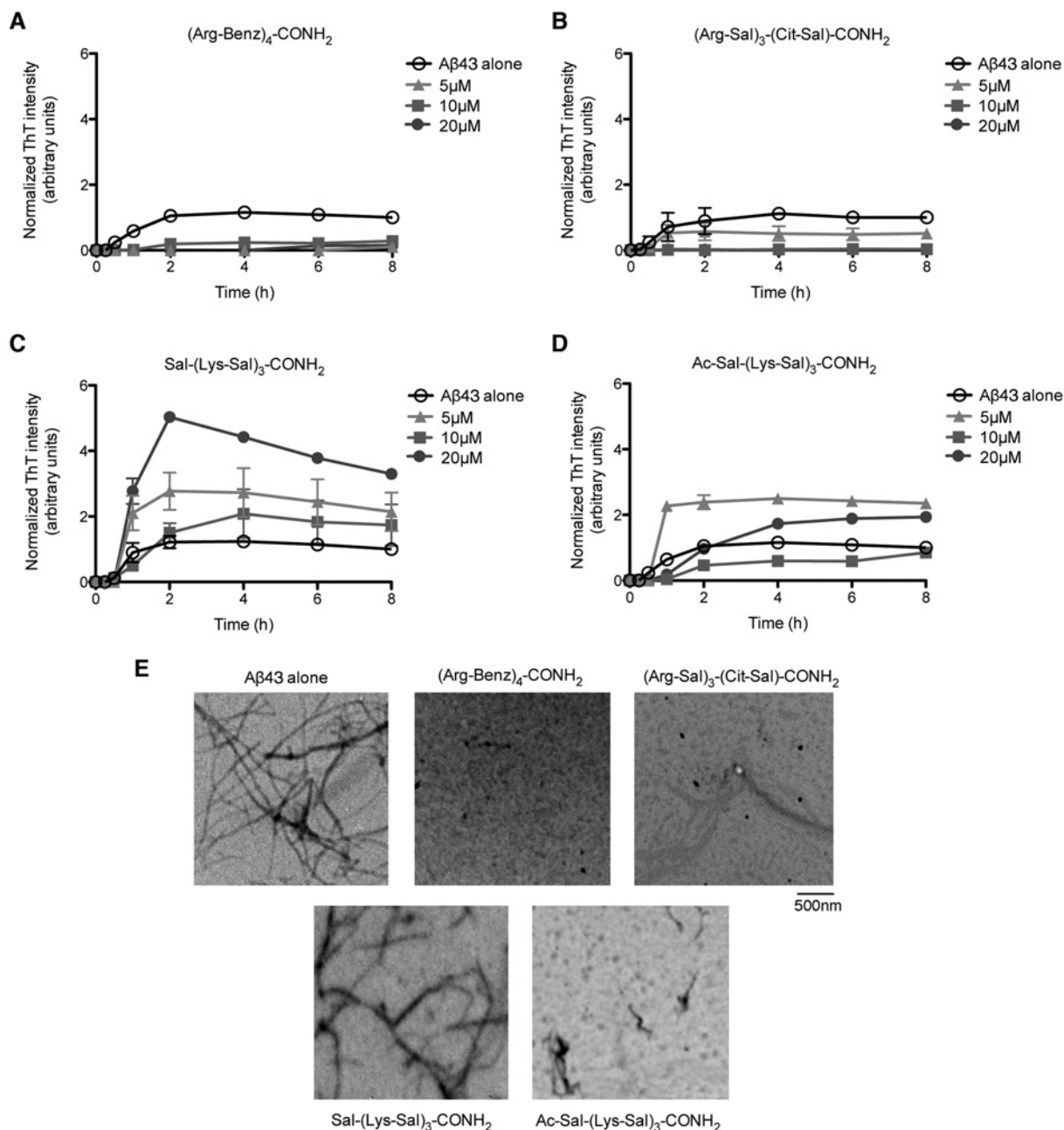


Figure 7 $(\text{Arg-Benz})_4\text{-CONH}_2$ and $(\text{Arg-Sal})_3\text{-(Cit-Sal)-CONH}_2$ inhibit spontaneous Aβ43 fibrillization

(A–D) Aβ43 (5 μM) was incubated with agitation for 0–8 h at 25 °C in the absence (open circles) or presence of 5 μM (filled triangles), 10 μM (filled squares) or 20 μM (filled circles) $(\text{Arg-Benz})_4\text{-CONH}_2$ (A), $(\text{Arg-Sal})_3\text{-(Cit-Sal)-CONH}_2$ (B), $\text{Sal-(Lys-Sal)}_3\text{-CONH}_2$ (C) or $\text{Ac-Sal-(Lys-Sal)}_3\text{-CONH}_2$ (D). Aβ43 fibrillization was assessed by ThT fluorescence. Values represent means ± S.E.M. ($n = 3$). (E) Aβ43 (5 μM) was incubated with agitation for 4 h at 25 °C in the absence or presence of the indicated foldamer (10 μM). Aβ43 fibrillization was assessed by EM. Scale bar, 500 nm.

$(\text{Arg-Benz})_4\text{-CONH}_2$, $(\text{Arg-Sal})_3\text{-(Cit-Sal)-CONH}_2$ and $\text{Ac-Sal-(Lys-Sal)}_3\text{-CONH}_2$ did not inhibit FUS aggregation (Figure 5B). Interestingly, $\text{Sal-(Lys-Sal)}_3\text{-CONH}_2$ delayed FUS aggregation (Figure 5B). $\text{Sal-(Lys-Sal)}_3\text{-CONH}_2$ could serve as a lead foldamer to be optimized against FUS misfolding.

$(\text{Arg-Sal})_3\text{-(Cit-Sal)-CONH}_2$ and $\text{Ac-Sal-(Lys-Sal)}_3\text{-CONH}_2$ inhibit seeded Aβ42 fibrillization

$(\text{Arg-Benz})_4\text{-CONH}_2$ and $\text{Sal-(Lys-Sal)}_3\text{-CONH}_2$ only inhibited seeded Aβ42 fibrillization when present at a 4-fold molar excess

over Aβ42 (Figures 6A and 6C, filled circles; Figure 6E). Even at this high concentration, some fibrillization occurred in the presence of $(\text{Arg-Benz})_4\text{-CONH}_2$ (Figure 6A, filled circles) but was very limited by $\text{Sal-(Lys-Sal)}_3\text{-CONH}_2$ (Figure 6C, filled circles). Thus, $(\text{Arg-Benz})_4\text{-CONH}_2$ and $\text{Sal-(Lys-Sal)}_3\text{-CONH}_2$ are more potent inhibitors of spontaneous Aβ42 fibrillization (Figures 4A and 4C) than seeded Aβ42 fibrillization (Figures 6A and 6C). $(\text{Arg-Benz})_4\text{-CONH}_2$ and $\text{Sal-(Lys-Sal)}_3\text{-CONH}_2$ likely preferentially inhibit the rearrangement of Aβ42 oligomers into fibril-nucleating species [22]. Once Aβ42 fibrils have formed,

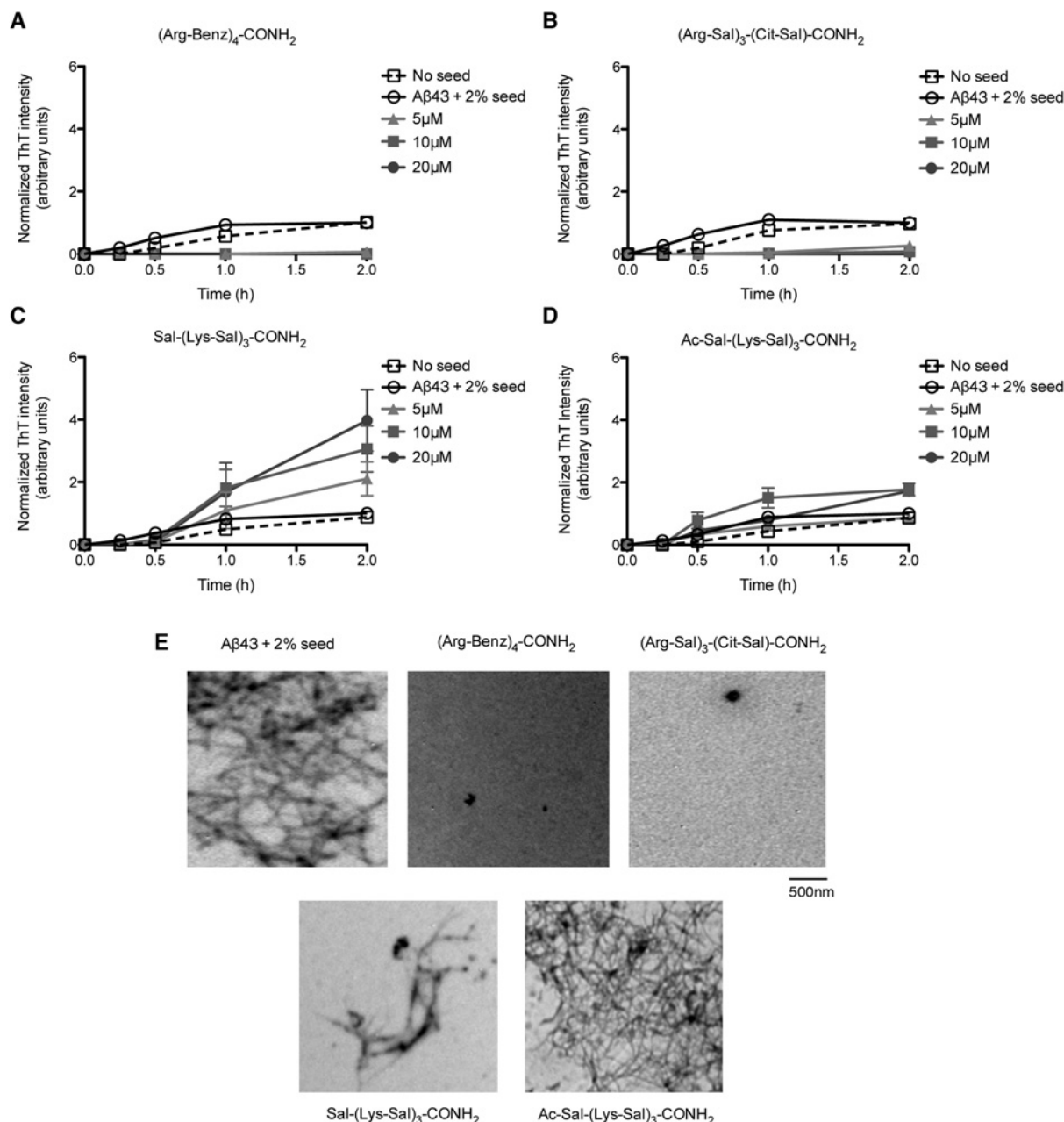


Figure 8 Foldamers (Arg-Benz)₄-CONH₂ and (Arg-Sal)₃-(Cit-Sal)-CONH₂ inhibit seeded A β 43 fibrillization

(A–D) A β 43 (5 μ M) was incubated with agitation for 0–2 h at 25 °C without (open squares) or with A β 43 fibril seed (0.1 μ M monomer) in the absence (open circles) or presence of 5 μ M (filled triangles), 10 μ M (filled squares) or 20 μ M (filled circles) (Arg-Benz)₄-CONH₂ (A), (Arg-Sal)₃-(Cit-Sal)-CONH₂ (B), Sal-(Lys-Sal)₃-CONH₂ (C) or Ac-Sal-(Lys-Sal)₃-CONH₂ (D). A β 43 fibrillization was assessed by ThT fluorescence. Values represent means \pm S.E.M. ($n = 3$). (E) A β 43 (5 μ M) plus A β 43 fibril seed (0.1 μ M monomer) was incubated with agitation for 4 h at 25 °C plus or minus the indicated foldamer (10 μ M). A β 42 fibrillization was assessed by EM. Scale bar, 500 nm.

(Arg-Benz)₄-CONH₂ and Sal-(Lys-Sal)₃-CONH₂ have reduced ability to inhibit assembly.

Ac-Sal-(Lys-Sal)₃-CONH₂ and (Arg-Sal)₃-(Cit-Sal)-CONH₂ inhibited seeded A β 42 fibrillization at all concentrations tested (Figures 6B, 6D and 6E). (Arg-Sal)₃-(Cit-Sal)-CONH₂ was more potent with an IC₅₀ of \sim 2.5 μ M (Figures 6B, 6D and 6E). Thus, Ac-Sal-(Lys-Sal)₃-CONH₂ and (Arg-Sal)₃-(Cit-Sal)-CONH₂ inhibit A β 42 fibrillization even after formation of species that nucleate fibrillization.

(Arg-Benz)₄-CONH₂ and (Arg-Sal)₃-(Cit-Sal)-CONH₂ inhibit spontaneous A β 43 fibrillization

It is unknown whether inhibitors that target A β 42 will also be active against A β 43. In the absence of foldamer, A β 43 fibrillization assembled more rapidly than A β 42 (Figures 4A–4D, and 7A–7D). Sal-(Lys-Sal)₃-CONH₂ and Ac-Sal-(Lys-Sal)₃-CONH₂ did not block spontaneous A β 43 fibrillization (Figures 7C–7E). Indeed, Sal-(Lys-Sal)₃-CONH₂ enabled A β 43

fibrils to form that exhibited higher ThT fluorescence (Figures 7C and 7E) and sedimentation analysis revealed that equal quantities of A β 43 formed fibrils (results not shown). Thus, Sal-(Lys-Sal)₃-CONH₂ does not stimulate A β 43 fibrillization. Rather, A β 43 may access a different amyloid strain in the presence of Sal-(Lys-Sal)₃-CONH₂. These findings suggest that potent inhibitors of spontaneous A β 42 fibrillization may not inhibit spontaneous A β 43 fibrillization. By contrast, (Arg-Benz)₄-CONH₂ and (Arg-Sal)₃-(Cit-Sal)-CONH₂ blocked spontaneous A β 43 fibrillization (Figures 7A, 7B and E). In both cases, small oligomers were the major species (Figure 7E). The IC₅₀ of (Arg-Sal)₃-(Cit-Sal)-CONH₂ was \sim 3.1 μ M (Figures 7A and 7B).

(Arg-Benz)₄-CONH₂ and (Arg-Sal)₃-(Cit-Sal)-CONH₂ inhibit seeded A β 43 fibrillization

A β 43 fibrils eliminated the lag phase of A β 43 assembly (Figures 8A–8D, compare open squares and open circles). Sal-(Lys-Sal)₃-CONH₂ and Ac-Sal-(Lys-Sal)₃-CONH₂ did not inhibit seeded A β 43 fibrillization (Figures 8C–8E). Sal-(Lys-Sal)₃-CONH₂ enabled A β 43 to access fibrillar forms that generated a higher ThT fluorescence signal, perhaps indicative of a distinct A β 43 amyloid strain (Figure 8C). By contrast, (Arg-Benz)₄-CONH₂ and (Arg-Sal)₃-(Cit-Sal)-CONH₂ blocked seeded A β 43 fibrillization (Figures 8A, 8B and 8E). The IC₅₀ of (Arg-Sal)₃-(Cit-Sal)-CONH₂ against seeded A β 43 fibrillization was \sim 1.7 μ M.

Foldamers inhibit A β 42 and A β 43 fibrillization under different assembly conditions

Next, we established that foldamers inhibited spontaneous and seeded A β 42 and A β 43 fibrillization under different assembly conditions, which might support formation of different amyloid strains. Thus, we avoided DMSO in A β preparation and assembled in a higher pH buffer. Under these conditions, a negative control foldamer, (Cit-Sal)₄-CONH₂, had no effect (Figure 9). By contrast, (Arg-Benz)₄-CONH₂, (Arg-Sal)₃-(Cit-Sal)-CONH₂, Sal-(Lys-Sal)₃-CONH₂ and Ac-Sal-(Lys-Sal)₃-CONH₂ inhibited spontaneous and seeded A β 42 fibrillization (Figure 9), whereas only (Arg-Benz)₄-CONH₂ and (Arg-Sal)₃-(Cit-Sal)-CONH₂ inhibited spontaneous and seeded A β 43 fibrillization (Figure 9).

(Arg-Sal)₃-(Cit-Sal)-CONH₂ antagonizes formation of A11-reactive A β 42 and A β 43 oligomers

Could foldamers inhibit the formation of toxic A β 42 and A β 43 oligomers? To assess toxic A β 42 and A β 43 oligomer formation, we employed the conformation-specific A11 antibody, which specifically recognizes preamyloid oligomers formed by multiple proteins, including A β 42, but not monomers or fibrils [21]. We assessed formation of A11-reactive species at the start of spontaneous assembly (0 h), at the end of lag phase (0.5 h), and at the endpoint of fibrillization (4 h). In the absence of A β 42 and A β 43, no A11 immunoreactivity was observed (results not shown). For A β 42 and A β 43, A11-reactive conformers were scarce at the start of the reaction (Figure 10A, buffer controls, black bars), abundant at end of lag phase (Figure 10A, buffer controls, grey bars), and declined once fibrillization was complete (Figure 10A, buffer controls, white bars). A β 43 exhibited greater A11-immunoreactivity than A β 42 and appears more prone to accessing this toxic conformation (Figure 10A).

A negative control foldamer, (Cit-Sal)₄-CONH₂ (Figure 2), had no effect on the appearance and disappearance of A11-reactive

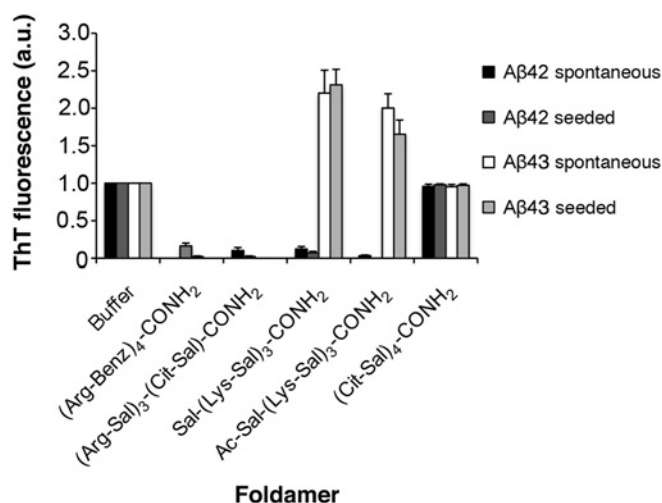


Figure 9 Foldamers inhibit A β 42 and A β 43 fibrillization under different assembly conditions

A β 42 or A β 43 (5 μ M) were incubated with agitation for 16 h at 25 °C without or with A β 42 fibril seed or A β 43 fibril seed (0.1 μ M monomer) plus or minus 20 μ M (Arg-Benz)₄-CONH₂, (Arg-Sal)₃-(Cit-Sal)-CONH₂, Sal-(Lys-Sal)₃-CONH₂, Ac-Sal-(Lys-Sal)₃-CONH₂ or (Cit-Sal)₄-CONH₂. Fibrillization was assessed by ThT fluorescence. Values represent means \pm S.E.M. ($n=3$).

A β 42 and A β 43 conformers (Figure 10A). (Arg-Benz)₄-CONH₂, Sal-(Lys-Sal)₃-CONH₂ and Ac-Sal-(Lys-Sal)₃-CONH₂ had no effect on the abundance of A11-reactive A β 42 or A β 43 oligomers after 0.5 h (Figure 10A, grey bars). Thus, these foldamers inhibit spontaneous A β 42 or A β 43 fibrillization without affecting the formation of A11-reactive conformers. Furthermore, after 4 h in the presence of (Arg-Benz)₄-CONH₂, Sal-(Lys-Sal)₃-CONH₂ and Ac-Sal-(Lys-Sal)₃-CONH₂, A11-reactive A β 42 species remained at higher levels and did not decline as much as they did in the absence of foldamer (Figure 10A, white bars). Thus, (Arg-Benz)₄-CONH₂, Sal-(Lys-Sal)₃-CONH₂, and Ac-Sal-(Lys-Sal)₃-CONH₂ stabilize A11-reactive conformers. (Arg-Benz)₄-CONH₂, but not Sal-(Lys-Sal)₃-CONH₂ or Ac-Sal-(Lys-Sal)₃-CONH₂, had a similar effect on A11-reactive A β 43 species (Figure 10A). By contrast, A11-reactive A β 43 species declined more extensively after 4 h in the presence of Sal-(Lys-Sal)₃-CONH₂ or Ac-Sal-(Lys-Sal)₃-CONH₂ (Figure 10A, white bars), which do not inhibit spontaneous A β 43 fibrillization (Figures 7C and 7D).

(Arg-Sal)₃-(Cit-Sal)-CONH₂ inhibited the formation of A11-reactive A β 42 and A β 43 conformers after 0.5 h (Figure 10A, grey bars). After 4 h, (Arg-Sal)₃-(Cit-Sal)-CONH₂ prevented further accumulation of A11-reactive A β 42 and A β 43 conformers (Figure 10A, white bars). Thus, (Arg-Sal)₃-(Cit-Sal)-CONH₂ inhibits fibrillization as well as toxic oligomer formation by A β 42 and A β 43. (Arg-Sal)₃-(Cit-Sal)-CONH₂ might inhibit A β 42 and A β 43 misfolding by a mechanism that is distinct to the other foldamers and arrests A β 42 and A β 43 misfolding prior to an A11-reactive oligomeric state.

(Arg-Sal)₃-(Cit-Sal)-CONH₂ inhibits formation of toxic A β 42 and A β 43 conformers

Next, we evaluated the relative toxicity of A β 42 and A β 43 conformers formed in the absence or presence of foldamers. We applied A β 42 and A β 43 conformers to SH-SY5Y neuroblastoma cells and assessed cell viability using MTT reduction and LDH release. Foldamers and buffer display little toxicity in the absence

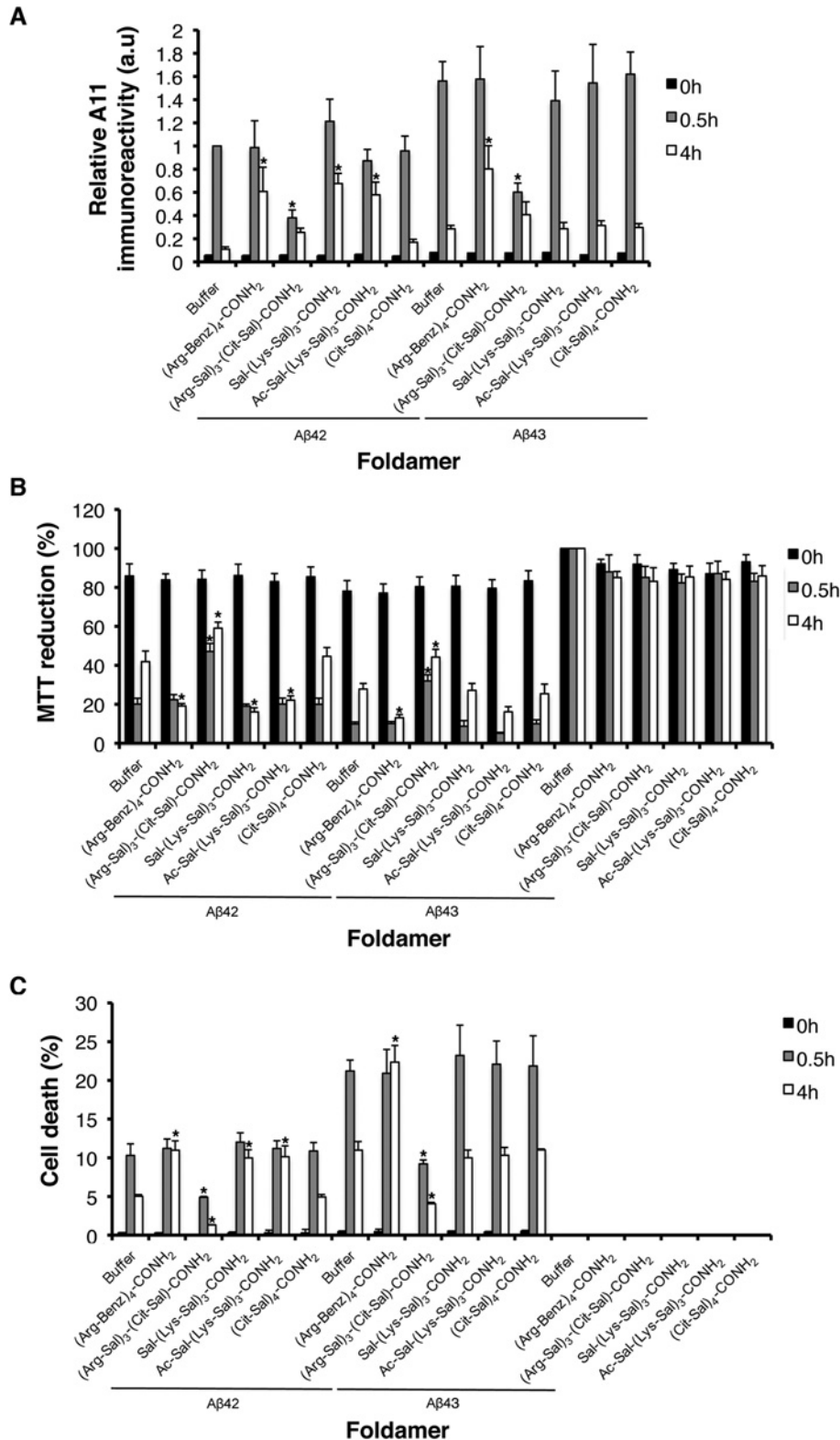


Figure 10 (Arg-Sal) $_3$ -(Cit-Sal)-CONH $_2$ inhibits formation of toxic A β 42 and A β 43 conformers

(A–C) A β 42 or A β 43 (5 μ M) was incubated at 25 $^{\circ}$ C with agitation for 0 h (black bars), 0.5 h (grey bars) or 4 h (white bars) in the absence or presence of 20 μ M (Arg-Benz) $_4$ -CONH $_2$, (Arg-Sal) $_3$ -(Cit-Sal)-CONH $_2$, Sal-(Lys-Sal) $_3$ -CONH $_2$, Ac-Sal-(Lys-Sal) $_3$ -CONH $_2$ or (Cit-Sal) $_4$ -CONH $_2$. At the indicated times, the amount of A11-reactive species present (A) or toxicity to SH-SY5Y neuroblastoma cells in culture was determined via MTT reduction (B) or LDH release (C). We also assessed the toxicity of buffer, (Arg-Benz) $_4$ -CONH $_2$, (Arg-Sal) $_3$ -(Cit-Sal)-CONH $_2$, Sal-(Lys-Sal) $_3$ -CONH $_2$, Ac-Sal-(Lys-Sal) $_3$ -CONH $_2$ or (Cit-Sal) $_4$ -CONH $_2$ alone (B and C). Values represent means \pm S.E.M. ($n = 3$). A one-way ANOVA with the post-hoc Dunnett's multiple comparisons test was used to compare A β 42 plus buffer to each A β 42 plus foldamer condition (* denotes $P < 0.05$). Likewise, a one-way ANOVA with the post-hoc Dunnett's multiple comparisons test was used to compare A β 43 plus buffer to each A β 43 plus foldamer condition (* denotes $P < 0.05$).

of $A\beta$ (Figures 10B and 10C, far right). In the absence of foldamer, $A\beta 42$ and $A\beta 43$ exhibited little toxicity after 0 h (Figures 10B and 10C), consistent with reduced A11 immunoreactivity at this time (Figure 10A). $A\beta 42$ and $A\beta 43$ were more toxic after 0.5 h of assembly than after 4 h (Figures 10B and 10C), indicating that conformers that accumulate at the end of lag phase are more toxic than mature fibrils. In the absence of foldamer, $A\beta 43$ conformers were generally more toxic than $A\beta 42$ conformers (Figures 10B and 10C). The negative control foldamer, (Cit-Sal)₄-CONH₂, had no effect on toxicity (Figures 10B and 10C). (Arg-Benz)₄-CONH₂, Sal-(Lys-Sal)₃-CONH₂ and Ac-Sal-(Lys-Sal)₃-CONH₂ had no effect on the toxicity of $A\beta 42$ conformers after 0.5 h of assembly (Figures 10B and 10C, grey bars), but after 4 h of assembly the toxicity of $A\beta 42$ conformers was enhanced (Figures 10B and 10C, white bars). Thus, (Arg-Benz)₄-CONH₂, Sal-(Lys-Sal)₃-CONH₂ and Ac-Sal-(Lys-Sal)₃-CONH₂ inhibit spontaneous $A\beta 42$ fibrillization such that more toxic conformers are maintained (Figures 10A–C). For $A\beta 43$, neither Sal-(Lys-Sal)₃-CONH₂ nor Ac-Sal-(Lys-Sal)₃-CONH₂ affected the toxicity of conformers after 0.5 h or 4 h (Figures 10B and 10C). However, as for $A\beta 42$, (Arg-Benz)₄-CONH₂ had no effect on the toxicity of $A\beta 43$ conformers after 0.5 h of assembly (Figures 10B and 10C, grey bars), but after 4 h the toxicity of $A\beta 43$ conformers was enhanced (Figures 10B and 10C, white bars). Thus, (Arg-Benz)₄-CONH₂ inhibits spontaneous $A\beta 43$ fibrillization in a manner that maintains toxic conformers (Figures 10A–10C).

(Arg-Sal)₃-(Cit-Sal)-CONH₂, which inhibited the formation of A11-reactive $A\beta 42$ and $A\beta 43$ conformers after 0.5 h (Figure 10A, grey bars), also partially reduced the toxicity of $A\beta 42$ and $A\beta 43$ conformers at this time (Figures 10B and 10C, grey bars) and at 4 h (Figures 10B and 10C, white bars). Although $A\beta 42$ and $A\beta 43$ conformers still conferred toxicity in comparison with buffer controls, (Arg-Sal)₃-(Cit-Sal)-CONH₂ was the only foldamer that antagonized $A\beta 42$ and $A\beta 43$ toxicity.

(Arg-Sal)₃-(Cit-Sal)-CONH₂ inhibits spontaneous and seeded $A\beta 42$ and $A\beta 43$ fibrillization and reduces accumulation of toxic $A\beta 42$ and $A\beta 43$ conformers. This combination of properties could have therapeutic potential for three reasons. First, (Arg-Sal)₃-(Cit-Sal)-CONH₂ antagonizes $A\beta 42$ as well as $A\beta 43$, which is an often overlooked but highly toxic $A\beta$ species [13–16]. Secondly, (Arg-Sal)₃-(Cit-Sal)-CONH₂ inhibits the formation of toxic $A\beta 42$ and $A\beta 43$ conformers, which could reduce localized neurodegeneration [65]. Thirdly, (Arg-Sal)₃-(Cit-Sal)-CONH₂ inhibits seeded $A\beta 42$ and $A\beta 43$ assembly, which could prevent the spreading of $A\beta$ pathology throughout the brain in AD [29–31]. Further studies are needed to assess the utility of (Arg-Sal)₃-(Cit-Sal)-CONH₂ against $A\beta$ misfolding and toxicity in the metazoan nervous system.

Future studies will reveal the mechanisms by which foldamers antagonize $A\beta$ -misfolding. Foldamers have amides oriented appropriately (Figure 2) to block growth from fibril ends during seeded polymerization. They are also relatively flat and aromatic (Figure 2) and might antagonize secondary nucleation by binding to the lateral surface of fibrils. Foldamer insertion into molten oligomers could inhibit rearrangement events required for nucleation during spontaneous assembly. Differences in the ability of specific foldamers to inhibit $A\beta 42$ fibrillization compared with $A\beta 43$ fibrillization probably reflect differential antagonism of events driven by the additional C-terminal steric zipper hexapeptide (G³⁸VVIAT⁴³) of $A\beta 43$.

Aromatic foldamers could be useful amyloidogenesis inhibitors for various disease-associated proteins. Indeed, another class of aromatic foldamer inhibits amylin fibrillization, which is connected to Type 2 diabetes [66]. Thus, foldamers await further development to antagonize protein misfolding in several settings.

AUTHOR CONTRIBUTION

Conceived and designed the experiments: Katelyn Seither, Heather McMahon, Nikita Singh, Hejia Wang, Mimi Cushman-Nick, Geronda Montalvo, William DeGrado and James Shorter. Performed the experiments: Katelyn Seither, Heather McMahon, Nikita Singh, Hejia Wang, Mimi Cushman-Nick and James Shorter. Analysed the data: Katelyn Seither, Heather McMahon, Nikita Singh, Hejia Wang, Mimi Cushman-Nick, Geronda Montalvo, William DeGrado and James Shorter. Contributed key reagents/materials: Geronda Montalvo and William DeGrado. Wrote the paper: Katelyn Seither, William DeGrado and James Shorter.

FUNDING

This work was supported by the National Institutes of Health [grant numbers T32AG000255 and F31NS067890 (to M.C.N.), GM54616 (to W.F.D.), DP2OD002177 (to J.S.), R21NS067354 (to J.S.), R21HD074510 (to J.S.) and R01GM099836 (to J.S.)]; National Science Foundation Materials Research Science and Engineering Centers grant to the Laboratory for Research on the Structure of Matter of the University of Pennsylvania [grant number DMR-1120901 (to W.F.D.)]; Muscular Dystrophy Association Research Award [grant number MDA277268]; Packard Center for ALS Research at Johns Hopkins University, Target ALS and an Ellison Medical Foundation New Scholar in Aging Award (to J.S.).

REFERENCES

- Cushman, M., Johnson, B. S., King, O. D., Gitler, A. D. and Shorter, J. (2010) Prion-like disorders: blurring the divide between transmissibility and infectivity. *J. Cell Sci.* **123**, 1191–1201 [CrossRef PubMed](#)
- Eisenberg, D. and Jucker, M. (2012) The amyloid state of proteins in human diseases. *Cell* **148**, 1188–1203 [CrossRef PubMed](#)
- Bieschke, J., Herbst, M., Wiglenda, T., Friedrich, R. P., Boeddrich, A., Schiele, F., Kleckers, D., Lopez del Amo, J. M., Grüning, B. A., Wang, Q. et al. (2012) Small-molecule conversion of toxic oligomers to nontoxic β -sheet-rich amyloid fibrils. *Nat. Chem. Biol.* **8**, 93–101 [CrossRef](#)
- Wang, H., Duenwald, M. L., Roberts, B. E., Rozeboom, L. M., Zhang, Y. L., Steele, A. D., Krishnan, R., Su, L. J., Griffin, D., Mukhopadhyay, S. et al. (2008) Direct and selective elimination of specific prions and amyloids by 4,5-dianilinothiophthalimide and analogs. *Proc. Natl. Acad. Sci. U.S.A.* **105**, 7159–7164 [CrossRef PubMed](#)
- Ehrnhoefer, D. E., Bieschke, J., Boeddrich, A., Herbst, M., Masino, L., Lurz, R., Engemann, S., Pastore, A. and Wanker, E. E. (2008) EGGC redirects amyloidogenic polypeptides into unstructured, off-pathway oligomers. *Nat. Struct. Mol. Biol.* **15**, 558–566 [CrossRef PubMed](#)
- Blanchard, B. J., Chen, A., Rozeboom, L. M., Stafford, K. A., Weigle, P. and Ingram, V. M. (2004) Efficient reversal of Alzheimer's disease fibril formation and elimination of neurotoxicity by a small molecule. *Proc. Natl. Acad. Sci. U.S.A.* **101**, 14326–14332 [CrossRef PubMed](#)
- Roberts, B. E. and Shorter, J. (2008) Escaping amyloid fate. *Nat. Struct. Mol. Biol.* **15**, 544–546 [CrossRef PubMed](#)
- Bulawa, C. E., Connelly, S., Devit, M., Wang, L., Weigel, C., Fleming, J. A., Packman, J., Powers, E. T., Wiseman, R. L., Foss, T. R. et al. (2012) Tafamidis, a potent and selective transthyretin kinetic stabilizer that inhibits the amyloid cascade. *Proc. Natl. Acad. Sci. U.S.A.* **109**, 9629–9634 [CrossRef PubMed](#)
- Nencetti, S., Rossello, A. and Orlandini, E. (2013) Tafamidis (Vyndaqel): a light for FAP patients. *ChemMedChem* **8**, 1617–1619
- Dasilva, K. A., Shaw, J. E. and McLaurin, J. (2010) Amyloid-beta fibrillogenesis: structural insight and therapeutic intervention. *Exp. Neurol.* **223**, 311–321 [CrossRef PubMed](#)
- Goedert, M. and Spillantini, M. G. (2006) A century of Alzheimer's disease. *Science* **314**, 777–781 [CrossRef PubMed](#)
- Holtzman, D. M., Morris, J. C. and Goate, A. M. (2011) Alzheimer's disease: the challenge of the second century. *Sci. Transl. Med.* **3**, 77sr71
- Saito, T., Suemoto, T., Brouwers, N., Slegers, K., Funamoto, S., Mihira, N., Matsuba, Y., Yamada, K., Nilsson, P., Takano, J. et al. (2011) Potent amyloidogenicity and pathogenicity of $A\beta 43$. *Nat. Neurosci.* **14**, 1023–1032 [CrossRef PubMed](#)
- Zou, K., Liu, J., Watanabe, A., Hiraga, S., Liu, S., Tanabe, C., Maeda, T., Terayama, Y., Takahashi, S., Michikawa, M. and Komano, H. (2013) $A\beta 43$ is the earliest-depositing $A\beta$ species in APP transgenic mouse brain and is converted to $A\beta 41$ by two active domains of ACE. *Am. J. Pathol.* **182**, 2322–2331 [CrossRef PubMed](#)
- Sandebing, A., Welander, H., Winblad, B., Graff, C. and Tjernberg, L. O. (2013) The pathogenic $A\beta 43$ is enriched in familial and sporadic Alzheimer disease. *PLoS ONE* **8**, e55847 [CrossRef PubMed](#)
- Welander, H., Fränberg, J., Graff, C., Sundström, E., Winblad, B. and Tjernberg, L. O. (2009) $A\beta 43$ is more frequent than $A\beta 40$ in amyloid plaque cores from Alzheimer disease brains. *J. Neurochem.* **110**, 697–706 [CrossRef PubMed](#)

- 17 Yan, Y. and Wang, C. (2007) Abeta40 protects non-toxic Abeta42 monomer from aggregation. *J. Mol. Biol.* **369**, 909–916 [CrossRef PubMed](#)
- 18 Kim, J., Onstead, L., Randle, S., Price, R., Smithson, L., Zwizinski, C., Dickson, D. W., Golde, T. and McGowan, E. (2007) Abeta40 inhibits amyloid deposition *in vivo*. *J. Neurosci.* **27**, 627–633 [CrossRef PubMed](#)
- 19 Colletier, J. P., Laganowsky, A., Landau, M., Zhao, M., Soriaga, A. B., Goldschmidt, L., Flot, D., Cascio, D., Sawaya, M. R. and Eisenberg, D. (2011) Molecular basis for amyloid- β polymorphism. *Proc. Natl. Acad. Sci. U.S.A.* **108**, 16938–16943 [CrossRef PubMed](#)
- 20 Jarrett, J. T., Berger, E. P. and Lansbury, Jr, P. T. (1993) The carboxy terminus of the beta amyloid protein is critical for the seeding of amyloid formation: implications for the pathogenesis of Alzheimer's disease. *Biochemistry* **32**, 4693–4697 [CrossRef PubMed](#)
- 21 Kaye, R., Head, E., Thompson, J. L., McIntire, T. M., Milton, S. C., Cotman, C. W. and Glabe, C. G. (2003) Common structure of soluble amyloid oligomers implies common mechanism of pathogenesis. *Science* **300**, 486–489 [CrossRef PubMed](#)
- 22 Lee, J., Culyba, E. K., Powers, E. T. and Kelly, J. W. (2011) Amyloid- β forms fibrils by nucleated conformational conversion of oligomers. *Nat. Chem. Biol.* **7**, 602–609 [CrossRef PubMed](#)
- 23 Harper, J. D., Wong, S. S., Lieber, C. M. and Lansbury, P. T. (1997) Observation of metastable Abeta amyloid protofibrils by atomic force microscopy. *Chem. Biol.* **4**, 119–125 [CrossRef PubMed](#)
- 24 Ladiwala, A. R., Litt, J., Kane, R. S., Aucoin, D. S., Smith, S. O., Ranjan, S., Davis, J., Van Nostrand, W. E. and Tessier, P. M. (2012) Conformational differences between two amyloid beta oligomers of similar size and dissimilar toxicity. *J. Biol. Chem.* **287**, 24765–24773 [CrossRef PubMed](#)
- 25 Stroud, J. C., Liu, C., Teng, P. K. and Eisenberg, D. (2012) Toxic fibrillar oligomers of amyloid- β have cross- β structure. *Proc. Natl. Acad. Sci. U.S.A.* **109**, 7717–7722 [CrossRef PubMed](#)
- 26 Lesné, S., Koh, M. T., Kotilinek, L., Kaye, R., Glabe, C. G., Yang, A., Gallagher, M. and Ashe, K. H. (2006) A specific amyloid- β protein assembly in the brain impairs memory. *Nature* **440**, 352–357 [CrossRef PubMed](#)
- 27 Bitan, G., Lomakin, A. and Teplow, D. B. (2001) Amyloid beta-protein oligomerization: prenucleation interactions revealed by photo-induced cross-linking of unmodified proteins. *J. Biol. Chem.* **276**, 35176–35184 [CrossRef PubMed](#)
- 28 Harper, J. D., Lieber, C. M. and Lansbury, Jr, P. T. (1997) Atomic force microscopic imaging of seeded fibril formation and fibril branching by the Alzheimer's disease amyloid- β protein. *Chem. Biol.* **4**, 951–959 [CrossRef PubMed](#)
- 29 Jucker, M. and Walker, L. C. (2013) Self-propagation of pathogenic protein aggregates in neurodegenerative diseases. *Nature* **501**, 45–51 [CrossRef PubMed](#)
- 30 Eisele, Y. S., Obermüller, U., Heilbronner, G., Baumann, F., Kaeser, S. A., Wolburg, H., Walker, L. C., Staufenbiel, M., Heikenwalder, M. and Jucker, M. (2010) Peripherally applied Abeta-containing inoculates induce cerebral beta-amyloidosis. *Science* **330**, 980–982 [CrossRef PubMed](#)
- 31 Meyer-Luehmann, M., Coomaraswamy, J., Bolmont, T., Kaeser, S., Schaefer, C., Kilger, E., Neuenschwander, A., Abramowski, D., Frey, P., Jaton, A. L. et al. (2006) Exogenous induction of cerebral beta-amyloidogenesis is governed by agent and host. *Science* **313**, 1781–1784 [CrossRef PubMed](#)
- 32 Cohen, S. I., Linse, S., Luheshi, L. M., Hellstrand, E., White, D. A., Rajah, L., Otzen, D. E., Vendruscolo, M., Dobson, C. M. and Knowles, T. P. (2013) Proliferation of amyloid- β 42 aggregates occurs through a secondary nucleation mechanism. *Proc. Natl. Acad. Sci. U.S.A.* **110**, 9758–9763 [CrossRef PubMed](#)
- 33 Cohen, S. I., Vendruscolo, M., Dobson, C. M. and Knowles, T. P. (2012) From macroscopic measurements to microscopic mechanisms of protein aggregation. *J. Mol. Biol.* **421**, 160–171 [CrossRef PubMed](#)
- 34 Meisl, G., Yang, X., Hellstrand, E., Frohm, B., Kirkegaard, J. B., Cohen, S. I., Dobson, C. M., Linse, S. and Knowles, T. P. (2014) Differences in nucleation behavior underlie the contrasting aggregation kinetics of the A β 40 and A β 42 peptides. *Proc. Natl. Acad. Sci. U.S.A.* **111**, 9384–9389 [CrossRef PubMed](#)
- 35 Lu, J. X., Qiang, W., Yau, W. M., Schwieters, C. D., Meredith, S. C. and Tycko, R. (2013) Molecular structure of beta-amyloid fibrils in Alzheimer's disease brain tissue. *Cell* **154**, 1257–1268 [CrossRef PubMed](#)
- 36 Petkova, A. T., Leapman, R. D., Guo, Z., Yau, W. M., Mattson, M. P. and Tycko, R. (2005) Self-propagating, molecular-level polymorphism in Alzheimer's beta-amyloid fibrils. *Science* **307**, 262–265 [CrossRef PubMed](#)
- 37 Aguzzi, A. and Gitler, A. D. (2013) A template for new drugs against Alzheimer's disease. *Cell* **154**, 1182–1184 [CrossRef PubMed](#)
- 38 Stöhr, J., Condello, C., Watts, J. C., Bloch, L., Oehler, A., Nick, M., DeArmond, S. J., Giles, K., DeGrado, W. F. and Prusiner, S. B. (2014) Distinct synthetic A β prion strains producing different amyloid deposits in bigenic mice. *Proc. Natl. Acad. Sci. U.S.A.* **111**, 10329–10334 [CrossRef PubMed](#)
- 39 Ladiwala, A. R., Dordick, J. S. and Tessier, P. M. (2011) Aromatic small molecules remodel toxic soluble oligomers of amyloid beta through three independent pathways. *J. Biol. Chem.* **286**, 3209–3218 [CrossRef PubMed](#)
- 40 Findeis, M. A., Musso, G. M., Arico-Muendel, C. C., Benjamin, H. W., Hundal, A. M., Lee, J. J., Chin, J., Kelley, M., Wakefield, J., Hayward, N. J. and Molineaux, S. M. (1999) Modified-peptide inhibitors of amyloid beta-peptide polymerization. *Biochemistry* **38**, 6791–6800 [CrossRef PubMed](#)
- 41 McKoy, A. F., Chen, J., Schupbach, T. and Hecht, M. H. (2012) A novel inhibitor of amyloid β (A β) peptide aggregation: from high throughput screening to efficacy in an animal model of Alzheimer disease. *J. Biol. Chem.* **287**, 38992–39000 [CrossRef PubMed](#)
- 42 Cheng, P. N., Liu, C., Zhao, M., Eisenberg, D. and Nowick, J. S. (2012) Amyloid β -sheet mimics that antagonize protein aggregation and reduce amyloid toxicity. *Nat. Chem.* **4**, 927–933 [CrossRef PubMed](#)
- 43 Evans, C. G., Wisen, S. and Gestwicki, J. E. (2006) Heat shock proteins 70 and 90 inhibit early stages of amyloid beta-(1–42) aggregation *in vitro*. *J. Biol. Chem.* **281**, 33182–33191 [CrossRef PubMed](#)
- 44 Ladiwala, A. R., Bhattacharya, M., Perchiacca, J. M., Cao, P., Raleigh, D. P., Abedini, A., Schmidt, A. M., Varkey, J., Langen, R. and Tessier, P. M. (2012) Rational design of potent domain antibody inhibitors of amyloid fibril assembly. *Proc. Natl. Acad. Sci. U.S.A.* **109**, 19965–19970 [CrossRef PubMed](#)
- 45 DeSantis, M. E., Leung, E. H., Sweeny, E. A., Jackrel, M. E., Cushman-Nick, M., Neuhaus-Follini, A., Vashist, S., Sochor, M. A., Knight, M. N. and Shorter, J. (2012) Operational plasticity enables Hsp104 to disaggregate diverse amyloid and nonamyloid clients. *Cell* **151**, 778–793 [CrossRef PubMed](#)
- 46 Gellman, S. H. (1998) Foldamers: a manifesto. *Acc. Chem. Res.* **31**, 173–180 [CrossRef](#)
- 47 Mensa, B., Kim, Y. H., Choi, S., Scott, R., Caputo, G. A. and DeGrado, W. F. (2011) Antibacterial mechanism of action of arylamide foldamers. *Antimicrob. Agents Chemother.* **55**, 5043–5053 [CrossRef PubMed](#)
- 48 Tew, G. N., Scott, R. W., Klein, M. L. and DeGrado, W. F. (2010) *De novo* design of antimicrobial polymers, foldamers, and small molecules: from discovery to practical applications. *Acc. Chem. Res.* **43**, 30–39 [CrossRef PubMed](#)
- 49 Choi, S., Clements, D. J., Pophristic, V., Ivanov, I., Vemparala, S., Bennett, J. S., Klein, M. L., Winkler, J. D. and DeGrado, W. F. (2005) The design and evaluation of heparin-binding foldamers. *Angew. Chem. Int. Ed. Engl.* **44**, 6685–6689 [CrossRef PubMed](#)
- 50 Goodman, C. M., Choi, S., Shandler, S. and DeGrado, W. F. (2007) Foldamers as versatile frameworks for the design and evolution of function. *Nat. Chem. Biol.* **3**, 252–262 [CrossRef PubMed](#)
- 51 Liu, C., Zhao, M., Jiang, L., Cheng, P. N., Park, J., Sawaya, M. R., Pensalfini, A., Gou, D., Berk, A. J., Glabe, C. G., Nowick, J. and Eisenberg, D. (2012) Out-of-register β -sheets suggest a pathway to toxic amyloid aggregates. *Proc. Natl. Acad. Sci. U.S.A.* **109**, 20913–20918 [CrossRef PubMed](#)
- 52 Zheng, J., Liu, C., Sawaya, M. R., Vadla, B., Khan, S., Woods, R. J., Eisenberg, D., Goux, W. J. and Nowick, J. S. (2011) Macrocyclic beta-sheet peptides that inhibit the aggregation of a tau-protein-derived hexapeptide. *J. Am. Chem. Soc.* **133**, 3144–3157 [CrossRef PubMed](#)
- 53 Kang, S. W., Gothard, C. M., Maitra, S., Wahab, A. T. and Nowick, J. S. (2007) A new class of macrocyclic receptors from iota-peptides. *J. Am. Chem. Soc.* **129**, 1486–1487 [CrossRef PubMed](#)
- 54 Guichard, G. and Huc, I. (2011) Synthetic foldamers. *Chem. Commun.* **47**, 5933–5941 [CrossRef PubMed](#)
- 55 Montalvo, G. L., Zhang, Y., Young, T. M., Costanzo, M. J., Freeman, K. B., Wang, J., Clements, D. J., Magavern, E., Kavash, R. W., Scott, R. W. et al. (2014) *De novo* design of self-assembling foldamers that inhibit heparin-protein interactions. *ACS Chem. Biol.* **9**, 967–975 [CrossRef PubMed](#)
- 56 Rahimi, F., Maiti, P. and Bitan, G. (2009) Photo-induced cross-linking of unmodified proteins (PICUP) applied to amyloidogenic peptides. *J. Vis. Exp.* **2009**, 1071 doi: 10.3791/1071 [CrossRef PubMed](#)
- 57 Roberts, B. E., Duennwald, M. L., Wang, H., Chung, C., Lopreiato, N. P., Sweeny, E. A., Knight, M. N. and Shorter, J. (2009) A synergistic small-molecule combination directly eradicates diverse prion strain structures. *Nat. Chem. Biol.* **5**, 936–946 [CrossRef PubMed](#)
- 58 Sun, Z., Diaz, Z., Fang, X., Hart, M. P., Chesi, A., Shorter, J. and Gitler, A. D. (2011) Molecular determinants and genetic modifiers of aggregation and toxicity for the ALS disease protein FUS/TLS. *PLoS Biol.* **9**, e1000614 [CrossRef PubMed](#)
- 59 Gazit, E. (2002) A possible role for pi-stacking in the self-assembly of amyloid fibrils. *FASEB J.* **16**, 77–83 [CrossRef PubMed](#)
- 60 Bieschke, J., Russ, J., Friedrich, R. P., Ehrnhoefer, D. E., Wobst, H., Neugebauer, K. and Wanker, E. E. (2010) ECGG remodels mature alpha-synuclein and amyloid-beta fibrils and reduces cellular toxicity. *Proc. Natl. Acad. Sci. U.S.A.* **107**, 7710–7715 [CrossRef PubMed](#)

- 61 Porat, Y., Abramowitz, A. and Gazit, E. (2006) Inhibition of amyloid fibril formation by polyphenols: structural similarity and aromatic interactions as a common inhibition mechanism. *Chem. Biol. Drug Des.* **67**, 27–37 [CrossRef PubMed](#)
- 62 Das, U., Hariprasad, G., Ethayathulla, A. S., Manral, P., Das, T. K., Pasha, S., Mann, A., Ganguli, M., Verma, A. K., Bhat, R. et al. (2007) Inhibition of protein aggregation: supramolecular assemblies of arginine hold the key. *PLoS One.* **2**, e1176 [CrossRef PubMed](#)
- 63 Shorter, J. (2010) Emergence and natural selection of drug-resistant prions. *Mol. Biosyst.* **6**, 1115–1130 [CrossRef PubMed](#)
- 64 King, O. D., Gitler, A. D. and Shorter, J. (2012) The tip of the iceberg: RNA-binding proteins with prion-like domains in neurodegenerative disease. *Brain Res.* **1462**, 61–80 [CrossRef PubMed](#)
- 65 Meyer-Luehmann, M., Spires-Jones, T. L., Prada, C., Garcia-Alloza, M., de Calignon, A., Rozkalne, A., Koenigsnecht-Talboo, J., Holtzman, D. M., Bacskai, B. J. and Hyman, B. T. (2008) Rapid appearance and local toxicity of amyloid-beta plaques in a mouse model of Alzheimer's disease. *Nature* **451**, 720–724 [CrossRef PubMed](#)
- 66 Kumar, S., Brown, M. A., Nath, A. and Miranker, A. D. (2014) Folded small molecule manipulation of islet amyloid polypeptide. *Chem. Biol.* **21**, 775–781 [CrossRef PubMed](#)

Received 6 December 2013/20 August 2014; accepted 21 August 2014

Published as BJ Immediate Publication 21 August 2014, doi:10.1042/BJ20131609